Optik - International Journal for Light and Electron Optics 195 (2019) 163105

Contents lists available at ScienceDirect

Optik

journal homepage: www.elsevier.com/locate/ijleo

Original research article

Dispersion of a surface plasmon polaritons in a thin dielectric films surrounded by a two graphene layers

A.S. Abramov*, D.A. Evseev, D.I. Sementsov

Ulyanovsk State University, 432017 Ulyanovsk, Russia

ARTICLE INFO

Keywords:
Surface plasmon-polariton
Symmetric and antisymmetric modes
Dispersion
Graphene
Slow surface waves
Negative and zero group velocity
Propagation length

ABSTRACT

In this work, we investigated the features of the propagation of surface plasmon-polariton modes with a frequencies $\omega = (10^{14}..10^{15})$rad/s with a symmetric and antisymmetric distribution of the electric field in the planar structure of a «graphene-thin dielectric film-graphene». They are received the dispersion characteristics for these types of modes. Also we found a spectral range, where the dispersion waves, phase and group velocity surface waves are most sensitive to change of a chemical potential of a graphene layers.

1. Introduction

Recently, the wave properties of thin film layered structures containing inclusions from graphene have been actively studied [1–5]. This is due to that the graphene is currently one of the most promising materials for optoelectronics. In particular, it was shown that in waveguided structures based on graphene surface plasmon polaritons of the infrared and terahertz range can be excited and propagated along the «graphene – thin film» interface [6–9]. And their wave characteristics are determined by both of the dispersion of the waveguided structure material parameters and the dispersion of the surface conductivity of graphene [9,10,30]. The control of dispersion characteristics can be realized by a change of the chemical potential (CP) of graphene, which depends on the external electric field and temperature [11,12].

Waveguided structures, in which propagation regime of slow waves is possible are significant interest for many applications of radiophysics [13–15]. It is shown, that in this structures may be organized the effective interaction between drift charge particles and propagated slow waves [16,17]. In particular, to create amplifiers and generators of the near and middle infrared range working on the principle of amplification of electromagnetic waves. Such interaction is based on the principle of operation of such microwave devices as klystron, traveling-wave- tube and particle accelerators [18]. It is important, that the effective interaction of the electromagnetic wave and charge carriers and, as a result, the realization of direct energy transfer from the current wave to the electromagnetic wave, is possible only if the carrier drift velocity in the material medium and the phase velocity of the surface electromagnetic wave are synchronized. This condition of approximate phase synchronism can be satisfied when the phase velocity of a wave is significant less than the speed of light in a vacuum [19].

In this moment the propagation of electromagnetic radiation in graphene-based structures has also been actively considered. In the work [20] in frequency region 18–42 THz for the periodically structure «graphene-dielectric» have been theoretically demonstrated a dynamically tunable dispersion of symmetric and antisymmetric surface plasmon polaritons. It have been shown that there are the strong coupling between modes with different symmetry. This strong coupling may be controlled by external gate voltage of

* Corresponding author.
E-mail address: aleksei_abramov@mail.ru (A.S. Abramov).

https://doi.org/10.1016/j.ijleo.2019.163105
Received 4 April 2019; Received in revised form 11 July 2019; Accepted 12 July 2019

graphene sheets or ribbon. Also authors analyzed the influence of structure's period on the dispersion of both type modes. Regimes of SPP propagation in mid infrared range in cylindrycal silica waveguide based on two graphene layers have investigated in Ref. [21]. The proposed cylindrical waveguide structure has a notable advantage for simultaneously achieving a larger propagation length of SPP for the fundamental mode and is 10 μm. Also, propagation length may be controlled by the level of Fermi energy in structure.

In this paper, we consider the influence of graphene layers deposited on surfaces of thin dielectric film on the its dispersion properties. We investigate a peculiarities of the propagation of surface modes with a symmetric and antisymmetric distribution of a wave field in a dielectric film. The possibility of controlling the phase and group velocity of the waveguide modes due to a change in the chemical potential (CP) of graphene layers is considered.

2. Material parameters

The features of the propagation of surface plasmon polaritons (SPP) will be investigated in a planar structure consisting of a thin dielectric layer of thickness d. The dielectric function of layer is constant and equal ε_d in the operating frequency range. The boundaries of the dielectric film $z = 0$ and $z = d$ surrounded by two graphene monolayers with surface electrical conductivities $\sigma_{1,3}$. The regarded structure is between two non-conducting media with dielectric constant ε_1 and ε_3. We assume that all materials of the structure are non-magnetic, i.e. their permeability is equal to one.

The frequency dependences of the real and imaginary parts of the surface conductivity of graphene in the Kubo model are determined by the following expressions [22,23]:

$$\frac{\sigma'}{\sigma_0} = \frac{1}{2} + \frac{1}{\pi} arctg\left(\frac{\hbar\omega - 2\mu}{2k_b T}\right),$$
$$\frac{\sigma''}{\sigma_0} = \frac{1}{2\pi}\frac{16k_b T}{\hbar\omega}\ln\left(2\cosh\left(\mu/2k_b T\right)\right) - \frac{1}{2\pi}\ln\left(\frac{(\hbar\omega + 2\mu)^2}{(\hbar\omega - 2\mu)^2 + (2k_b T)^2}\right). \quad (1)$$

Here are $\sigma_0 = e^2/4\hbar$ - static graphene conductivity, e—electron charge, $\hbar$—reduced Planck's constant, k_B—Boltzmann constant, T—temperature, $\mu = \hbar v_F\sqrt{\pi n_0}$—chemical potential, included charge carrier concentration n_0 and Fermi velocity v_F in graphene.

Fig. 1 shows the frequency dependences of the real (a) and imaginary parts (b) of the surface conductivity of graphene. This dependences were obtained in accordance with expressions (1) for room temperature and three different values of CP $\mu = (-0.1,\ 0,\ 0.1)$ eV (points, dashed and solid curves). For a negative CP $\mu = -0.1$ eV the real part is practically independent of frequency (point curve, a), and a characteristic resonance occurs at the frequency $\omega \simeq 3{\cdot}10^{14}$ rad/s in the imaginary part (point curve,

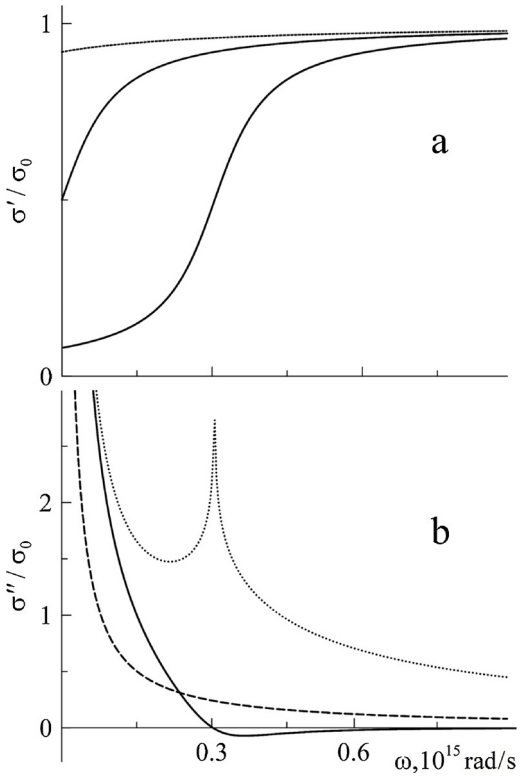

Fig. 1. Frequency dependencies of the real (a) and imaginary part (b) of the surface conductivity of graphene for three values of CP $\mu = (-0.1, 0.0, 0.1)$ eV (points, dashed and solid curves).

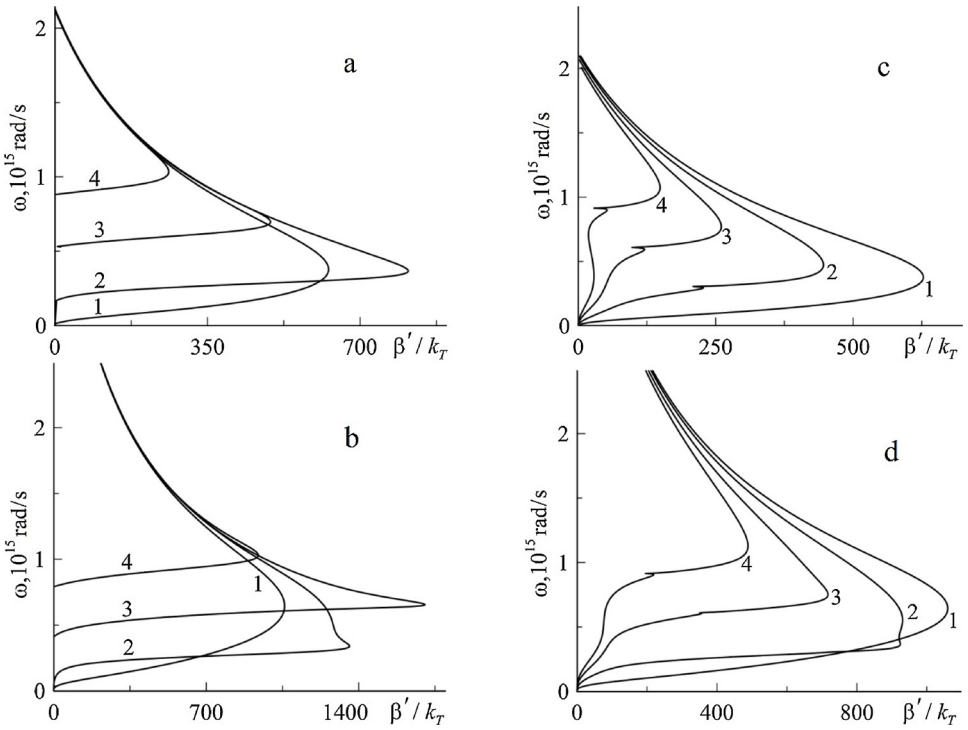

Fig. 2. Dispersion dependencies for symmetric (a, c) and antisymmetric (b, d) plasmon polaritons for CP values $\mu_2 = \mu_1 = 0.0,\ 0.1,\ 0.2,\ 0.3$ eV (a, b, curves 1–4) and $\mu_2 = -\mu_1 = 0.0,\ 0.1,\ 0.2,\ 0.3$ eV (c, d, curves 1–4). The thickness of a dielectric layer is $d = 10$ nm.

b). For a zero values of CP $\mu = 0.0$ eV an increase in frequency is accompanied by a growth and saturation of the real part σ' and the rapid decline of the imaginary part σ'' (dashed curves a, b). In case of a positive values graphene CP $\mu = 0.1$ eV the frequency dependences $\sigma'(\omega)$ is contained the region of rapid growth of the real part of the conductivity (solid curve, a) and the dependences $\sigma''(\omega)$ have a characteristic minimum of the imaginary part of graphene conductivity (solid curves a, b). The analysis shows that with increasing CP the area of growth of intrinsic conductivity σ' will shift to the high frequency region. The same displacement will have a minimum of the imaginary part of the conductivity σ''.

In the general case, graphene CP depends on the external electric field and temperature [12]. Often there is a situation where the value CP μ can be controlled by applying an external voltage to the plates of graphene. For example, for p-type graphene, the relationship between external voltage U_g and CP can be written as $\mu(U_g) = e(U_g - ep/c_g - \varphi_0)$, where p is the surface concentration of holes, c_g is the capacitance of a unit area of graphene, φ_0 is the residual electric potential [24]. It is shown that the negative and zero CP can be achieved by applying reverse and zero voltage respectively [11,25].

3. Dispersion equation

We will regard propagation of SPP with a TM polarization along the longitudinal axis x on the both interfaces of the media $z = 0$ and $z = d$. Wave field components of SPP are $F_\alpha = (E_x,\ H_y,\ E_z)$. Dependence their components on time and along x and transverse z coordinates may be written as:

$$F_\alpha(x, z, t) = F_\alpha(z)\exp[i(\omega t - \beta x)], \tag{2}$$

where $F_\alpha(z)$ is profile function of respective component of wave field, $\beta = \beta' + i\beta''$ is complex constant of propagation. The relationship between these components is determined by the equations:

$$\frac{\partial^2 E_x}{\partial z^2} - q_j^2 E_x = 0, \quad H_y = \frac{i}{k_0\varepsilon_j}\frac{\partial E_x}{\partial z}, \quad E_z = -\frac{\beta}{k_0\varepsilon_j}H_y, \tag{3}$$

here q_j is transverse components of a wave vector in each media ($j = 1,2,3$). In this case $q_{1,3} = \sqrt{\beta^2 - \varepsilon_{1,3}k_0^2}$ and $q_2 = \sqrt{\beta^2 - k_0^2\varepsilon_d}$ and $k_0 = \omega/c$, c is speed of light in vacuum.

In order to solve the boundary problem for SPP in considered structure it is necessary take into account the graphene conductivity on the each boundary of structure $z = 0,\ d$:

$$E_{1,3x} = E_{2x}, \quad H_{1,3y} - H_{2y} = \pm(4\pi/c)\sigma_{1,3}E_{1,3x}\,. \tag{4}$$

The dispersion equation for SPP in this structure is obtained from the condition of equality to zero of determinant of system Eq.

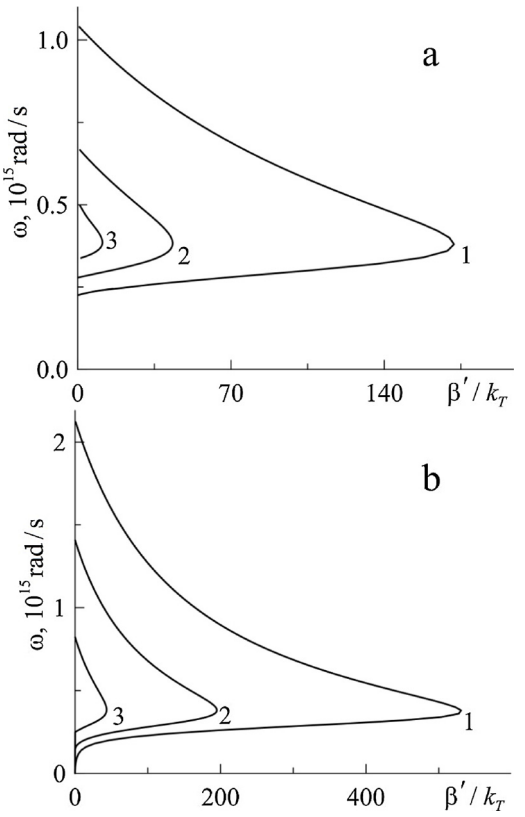

Fig. 3. Dispersion dependencies for symmetric (a) and antisymmetric (b) plasmon polaritons for three values of dielectric layer thicknesses $d = 20,\ 30,\ 50$ nm (curves 1–3). The CP of a graphene is $\mu = 0.1$ eV.

(4):

$$\exp(2q_2 d) = \frac{1 - \frac{\varepsilon_1 q_2}{\varepsilon_2 q_1} - i\frac{4\pi\sigma_1 q_2}{\varepsilon_2 c k_0}}{1 + \frac{\varepsilon_1 q_2}{\varepsilon_2 q_1} + i\frac{4\pi\sigma_1 q_2}{\varepsilon_2 c k_0}} \cdot \frac{1 - \frac{\varepsilon_3 q_2}{\varepsilon_2 q_3} - i\frac{4\pi\sigma_3 q_2}{\varepsilon_2 c k_0}}{1 + \frac{\varepsilon_3 q_2}{\varepsilon_2 q_3} + i\frac{4\pi\sigma_3 q_2}{\varepsilon_2 c k_0}}, \tag{5}$$

In Eq. (5) σ_1 and σ_3 are the surface conductivities of the upper and lower graphene layers. In the absence of graphene at the boundaries of the structure Eq. (5) is reduced to the standard dispersion relation for bulk modes in dielectric waveguide [26]. The dispersion relation (5) is simplified for case the same CP and therefore the same conductivities $\sigma_1 = \sigma_3 = \sigma$ and when dielectric constant of cover media is equals $\varepsilon_1 = \varepsilon_3 = \varepsilon$:

$$\exp(q_d d) = \left(1 - \frac{\varepsilon q_d}{\varepsilon_d q} - i\frac{4\pi\sigma q_d}{\varepsilon_d c k_0}\right) \Big/ \left(1 + \frac{\varepsilon q_d}{\varepsilon_d q} + i\frac{4\pi\sigma q_d}{\varepsilon_d c k_0}\right), \tag{6}$$

where $q_d = q_2$, $q = q_{1,3}$. In turn the Eq. (6) can be divided into two equations for surface symmetric and antisymmetric modes respectively:

$$\frac{q_d d}{2} + \operatorname{arctg}\frac{\gamma\, q_d}{\varepsilon_d q} = \pi m, \quad \frac{q_d d}{2} + \operatorname{arcctg}\frac{\gamma\, q_d}{\varepsilon_d q} = \pi m. \tag{7}$$

In relationships (7) parameter $\gamma = 1 + i4\pi\sigma q/ck_0$ is equal to one in absence of a graphene on the boundaries structure.

The dependence of the tangential component of the electric E_x and magnetic H_y fields of the SPP on the transverse coordinate z is written in the form:

$$E_x(z) = E_0 \begin{cases} e^{qz}, & z < 0, \\ \operatorname{ch}(q_d z) + (\varepsilon_d q\gamma/q_d)\operatorname{sh}(q_d z), & 0 < z < d, \\ [\operatorname{ch}(q_d d) + (\varepsilon_d q\gamma/q_d)\operatorname{sh}(q_d d)]e^{q(d-z)}, & z > d, \end{cases} \tag{8a}$$

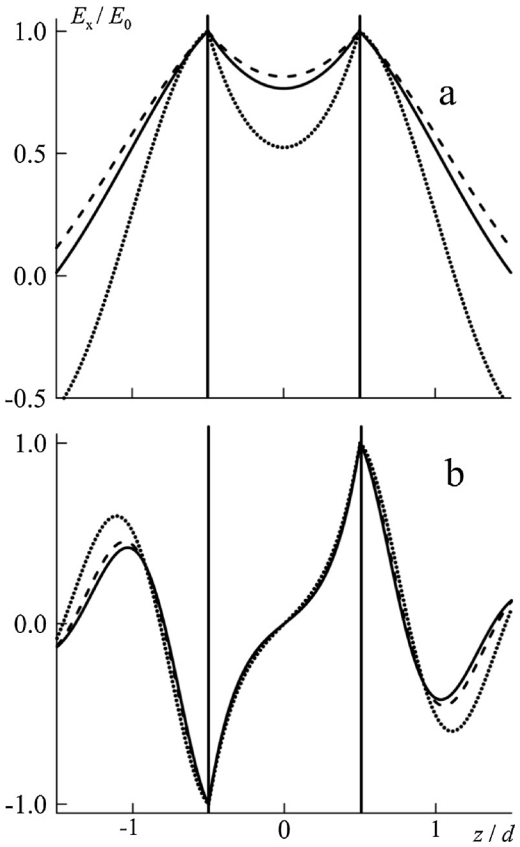

Fig. 4. The distribution of the electric field in the transverse coordinate for symmetric (a) and antisymmetric (b) SPP for three values of CP $\mu = (-0.1,\ 0.0,\ 0.1)$ eV (points, dashed and solid curves). Frequency of SPP is $\omega = 7.5{\cdot}10^{14}$ rad/s.

$$H_y(z) = \frac{iq_d E_0}{k_0 \varepsilon_d \gamma} \begin{cases} (q\varepsilon_d\gamma/q_d)\mathrm{e}^{qz}, & z < 0, \\ \gamma[\mathrm{sh}(q_d z) + (\varepsilon_d q\gamma/q_d)\mathrm{ch}(q_d z)], & 0 < z < d, \\ [\mathrm{sh}(q_d d) + (\varepsilon_d q\gamma/q_d)\mathrm{ch}(q_d d)]\mathrm{e}^{q(d-z)}, & z > d, \end{cases} \tag{8b}$$

here E_0 is amplitude of the electric field SPP on the boundary $z = 0$.

Below there are the results of a numerical analysis of the regime propagation of surface symmetric and antisymmetric modes in the considered structure.

4. Numerical analysis

We assume that the structure is in a vacuum and the dielectric constant of the central layer is $\varepsilon_d = 5$. Thickness of the thin films is taken equal $d = 10$ nm. The analysis is carried out for the spectral range $\omega = (0.3 - 1.5){\cdot}10^{15}$rad/s in which the change in the CP of graphene leads to significant changes in the propagation constant. In this case the control of the dispersion characteristics of the SPP is most effective. Fig. 2 shows the dispersion dependences $\omega(\beta')$, which are solutions of Eq. (7) for symmetric (a, c) and antisymmetric (b, d) modes. Here the propagation constant β' is normalized to the value $k_T = k_B T/\hbar c = 1.31{\cdot}10^3\,\mathrm{cm}^{-1}$. In this work the calculated CP values of graphene layers are assumed to be equal $\mu_1 = \mu_2 = 0,\ 0.1,\ 0.2,\ 0.3$ eV (curves 1–4, a, b) and $\mu_1 = -\mu_2 = 0,\ 0.1,\ 0.2,\ 0.3$ eV (curves 1–4, c, d). It is seen, that for antisymmetric modes (b, d) the region of change β' is almost twice the size of the corresponding region for symmetric modes (a, c). For case of $\mu_1 = -\mu_2$ on the dispersion curves there are the characteristic resonances appear associated with the resonances of the imaginary part of the graphene conductivity at the corresponding frequency (see Fig. 1b, points). This feature leads to the appearance of an additional frequency region in which the group velocity of the SPP can take zero and negative values. The position of the resonances can be controlled by changing the variation of CP. The analysis shows that surface waves are realized in the structure also for large values of CP $\mu > 0.3$ eV. In this case the spectral interval of their existence is shifted to the high frequency region, and the range of variation of the propagation constants is narrowed.

In Fig. 3 presents the dispersion dependences for symmetric (a) and antisymmetric (b) SPP for three different values of the thickness of the dielectric layer $d = 20,\ 30,\ 50$ nm (curves 1–3). The value of CP graphene is $\mu = 0.1$ eV. It can be seen that the region of existence of symmetric modes turns out to be much narrower than that of antisymmetric modes. In this case the region of existence of the surface mode sharply narrows both in the range of propagation constants and in the frequency range as the thickness of the

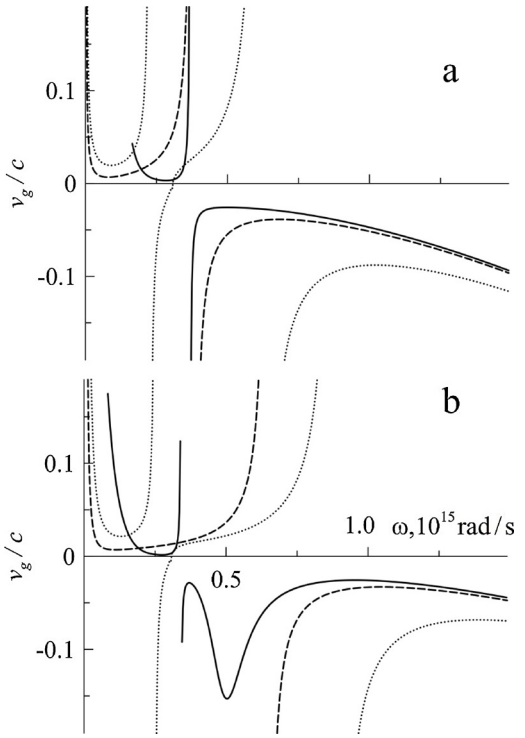

Fig. 5. Frequency dependences of group velocities for symmetric (a) and antisymmetric SPP for three values of CP $\mu = (-0.1, 0.0, 0.1)$ eV(points, dashed and solid curves).

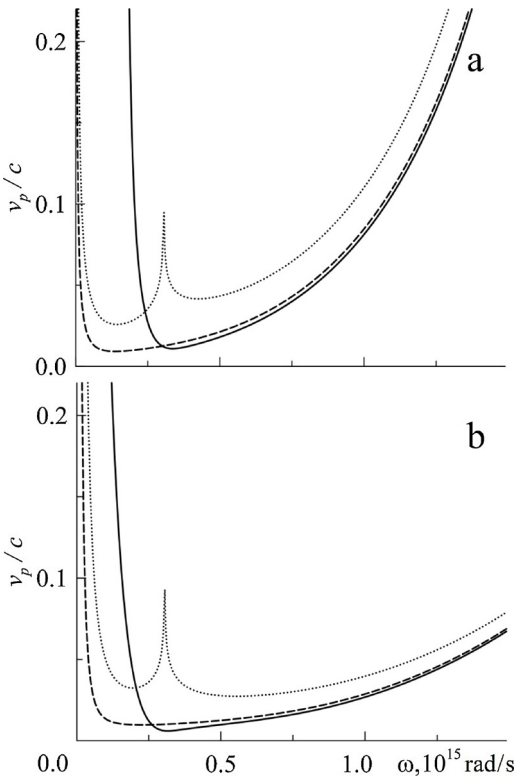

Fig. 6. Frequency dependences of phase velocities for symmetric (a) and antisymmetric SPP for three values of CP $\mu = (-0.1, 0.0, 0.1)$ eV(points, dashed and solid curves).

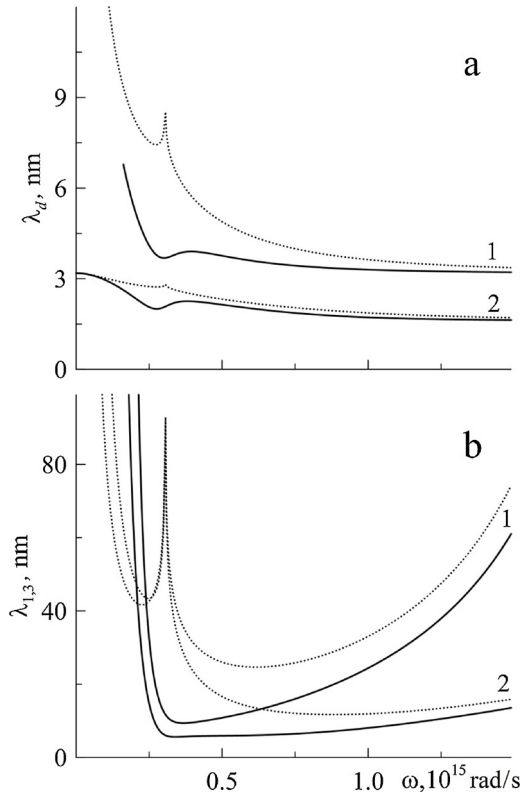

Fig. 7. Frequency dependencies of the penetration depth of SPP in the dielectric film (a) and coating media (b) for symmetric (curves 1) and antisymmetric (curves 2) SPP with values CP $\mu = (-0.1,\ 0.1)$ eV (points and solid curves).

dielectric layer increases.

In work [10] have been investigated multilayer structures containing graphene and dielectric layers. The relevant dispersion relations are received, it is demonstrated that tuning can be achieved by modifying the Fermi energy. It is shown, tunability of the graphene-dielectric heterostructures can be controlled by changing either the thickness of the dielectric layers or the number of graphene sheets employed.

Next we plot the distributions of the normalized amplitude of the electric field on the transverse coordinate of symmetric (a) and antisymmetric (b) surface modes for the values of CP $\mu = (-0.1,\ 0.0,\ 0.1)$ eV (points, dashed and solid curves) as shown in Fig. 4. This distributions are obtained according to expressions (8) at a SPP frequency $\omega = 7.5{\cdot}10^{14}$ rad/s. The change in CP of graphene leads to modification of the distribution of the SPP field in the structure, which is most noticeable for symmetric modes. We note that the symmetry of the distribution of the wave magnetic field is opposite to the symmetry of the distribution of the electric field in the structure. In work [27] were plotted the profiles of electric and magnetic fields in the graphene–metal waveguide for two values of applied voltage. It is found the SPP attenuation increases when applied voltage is adjusted from 6 to 7.76 V.

On the basis of the above dispersion dependences $\omega(\beta')$ we consider the behavior of the group velocities $V_g = d\omega/d\beta'$ and phase velocities $V_p = \omega/\beta'$ of SPP propagating in the structure. Fig. 5 shows the dependences $V_g(\omega)$ for symmetric and antisymmetric (a, b) surface modes for the previously chosen three CP values. For both types of surface modes, both positive and negative group velocities can be achieved in the considered frequency range. It can be seen that at the critical frequency ω_{cr}, which on the dispersion dependences corresponds to the maximum of the propagation constant β', the group velocity changes its sign. Up to the critical frequency the group velocity is positive, and the frequencies $\omega > \omega_{cr}$ are characterized by a negative group velocity of the SPP. The boundaries of the frequency range, in which the group velocity is negative expand with increasing CP of graphene. In a narrow region of frequencies close to critical the group velocity tends to infinity $V_g \to \infty$. An exception is the case $\mu = 0$ (points) for which when the sign of the group velocity changes in the resonance region, both types of modes are characterized by zero group velocity, i.e., the full stop of the SPP. For effective interaction of surface waves with carrier fluxes and other excitations in the structure must be conditions of phase synchronism between them. In order to phase synchronism conditions to be satisfied the phase velocity of the SPP must be close to the velocity of the carriers or excitations. On the Fig. 6 we plotted the dependences $V_p(\omega)$ for symmetric and antisymmetric (a, b) surface modes for the three previously chosen CP values. With the selected design parameters the minimum possible magnitude of phase velocity of SPP is achieved for antisymmetric modes with $\mu = 0.1$ eV (solid curve, b) and is $V_p/c \approx 0.012$. The frequency range in which small values of phase velocities of the SPP are achieved significantly expands at zero CP (dashed curves). Note that with increasing frequency starting from $\omega \simeq 5{\cdot}10^{14}$ rad/s, an increase in phase velocities is observed for both types of modes, however, for symmetric modes it is faster than for antisymmetric modes.

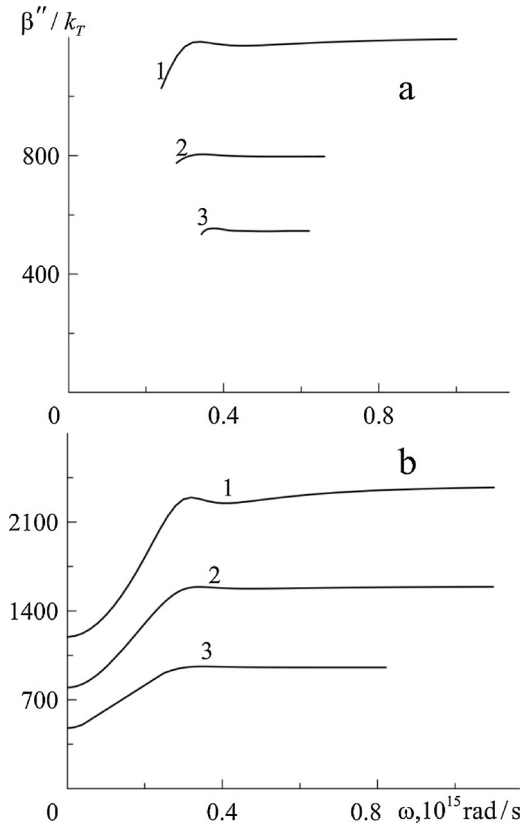

Fig. 8. Frequency dependencies of the imaginary part of the propagation constant for symmetric (a) and antisymmetric (b) SPP for thicknesses of 20, 30, and 50 nm (curves 1–3).

The deceleration of the surface modes and first waveguide modes was investigated in the structure of the «dielectric waveguide - monolayer graphene-covering medium» [4,28,29]. It is established that the value of the effective refractive index for the IR modes was close to 100. This indicates that the phase velocities of the propagating modes can be almost two orders of magnitude smaller than the speed of light in a vacuum.

Now we will consider the question of the penetration depth of the surface wave in the structure. Fig. 7 shows the frequency dependences of the penetration depth of the wave field in the dielectric film $\lambda_d = 1/q'_d$ (a) and in the coating medium $\lambda_{1,3} = 1/q'_{1,3}$ (b) with two values graphene CP $\mu = (-0.1,\ 0.1)$ eV (points and solid curves) for symmetric (curves 1) and antisymmetric (curves 2) surface modes. Analysis shows that the localization of the field in the dielectric film is significantly higher than in the vacuum. At the same time, the localization of antisymmetric modes is higher than symmetric modes, i.e., the penetration depth of occurrence for symmetric SPP at a fixed frequency is higher than the depth for antisymmetric SPP. A variation of the graphene CP also leads to a change in the penetration depth at a fixed frequency. This is most effective at frequencies $\omega = (0.2..0.5)\cdot 10^{15}$rad/s. Thus, the field of the symmetric mode is more concentrated in the volume of waveguide structure. Consequently, for the modes of this type the energy loss during propagation will be higher than for antisymmetric modes.

Very important for the practical use of surface waves is the question of the propagation length of SPP in a waveguide structure. Propagation length of SPP related to the imaginary part of the propagation constant by the ratio $l \approx 1/\beta''$. For the selected spectral range on the Fig. 8 we plotted the frequency dependences of the magnitude β'' for symmetric and antisymmetric (a, b) modes is obtained for the value of CP $\mu = 0.1$ eV and film thicknesses $d = 20,\ 30,\ 50$ nm (curves 1–3). It can be seen that in the region of existence of the SPP with increasing film thickness the damping decreases and, therefore, the length propagation increases. At that for symmetric modes the value should be practically twice as large as for antisymmetric ones with identical film thicknesses. For example, in work [31] for SPP from frequency range $\omega = (0.1..4.0)\cdot 10^{15}$rad/s also have been shown, that the absorption in structure and localization of SPP depend on the level of Fermi energy, hence and from CP. Additionally, absorption can be influenced by changing the material of the dielectric layer between the graphene sheets and its thickness.

However, the propagation length of the surface wave in the structure is extremely small and is comparable with the thickness of the waveguide layer. For comparison in the optical range the path length of the SPP in the structure based on nanometer metal thickness exceeds corresponding path length of SPP in graphene structure. Usually, propagation length of SPP in metal is from a few units to tens of microns [32]. However the use of graphene layers allows effectively manage by the characteristics of propagating SPP by the external electric fields and temperature.

Thereby to use the features indicated in the work in practice compensation of losses in the structure is necessary. This can be

realized, for example, by creating an effective interaction of the SPP field with the current pumping wave supplied to the structure in conditions close to phase synchronism.

5. Conclusion

In this work we investigated the propagation features of symmetric and antisymmetric plasmon polariton modes in a dielectric structure located between two graphene monolayers. It is shown that a change in CP graphene leads to a change in the dispersion of SPP in the structure. For antisymmetric modes there is a frequency range, which is characterized by a low phase velocity, which is almost two orders of magnitude different from the speed of light in a vacuum. For both types of field distribution the negative group velocity of the SPP is realized, and with increasing CP the boundaries of this interval expand. When a zero chemical potential is applied the zero group velocity of the OP can be occurred. It creates conditions for their further effective interaction with external pumping. This condition allows one to realize on the basis of the considered structure plasmon resonators with a high quality factor.

Nevertheless, the analysis shows that the length of the SPP in the waveguide structure is extremely small and does not exceed several nanometers. In this regard for the application of these wave features in practice, it is necessary to create additional conditions for amplifying attenuated in the structure of the SPP.

Acknowledgements

This work was supported by Department of Education and Science of Russia (project № 3.6825/BCh), Russian Scientific Found (project № 17-72-10135) and Russian Found of Fundamental Investigation (project № 18-42-730005).

References

[1] S. Xiao, X. Zhu, B.-H. Li, N.A. Mortensen, Graphene-plasmon polaritons: from fundamental properties to potential applications, Front. Phys. 11 (2016) 117801 https://link.springer.com/article/10.1007/s11467-016-0551-z.
[2] M. Sun, J. Tian, X. Lan, Zh. He, J. Liu, Transmission properties of two vertically coupled doublegraphene-coated nanowires integrated with substrate, Optik 185 (2019) 242–247, https://doi.org/10.1016/j.ijleo.2019.03.090.
[3] S. Khazaee, N. Granpayeh, Tunable multiple plasmon induced transparencies in parallel graphene sheets and its applications, Opt. Commun. 406 (2018) 199–204, https://doi.org/10.1016/j.optcom.2017.02.033.
[4] W. Xu, Z.H. Zhu, K. Liu, J.F. Zhang, X.D. Yuan, Q.S. Lu, S.Q. Qin, Dielectric loaded graphene plasmon waveguide, Opt. Express 23 (2015) 5147–5153, https://doi.org/10.1364/OE.23.005147.
[5] Yu Bludov, A. Ferreira, N. Peres, M. Vasilevskiy, A primer on in surface plasmon polaritons in graphene, Int. J. Mod. Phys. B 27 (2013) 1341001, https://doi.org/10.1142/S0217979213410014.
[6] P.I. Buslaev, I.V. Iorsh, I.V. Shadrivov, P.A. Belov, Yu S. Kivshar, Plasmons in waveguide structures formed by two graphene layers, JETP Lett. 97 (2013) 535–539, https://doi.org/10.1134/S0021364013090063.
[7] P. Burghignoli, Time-domain surface plasmon polaritons on a graphene sheet, Phys. Rev. B 97 (2018) 245418, https://doi.org/10.1103/PhysRevB.97.245418.
[8] C.H. Gan, Analysis of surface plasmon excitation at terahertz frequencies with highly doped graphene sheets via attenuated total reflection, Appl. Phys. Lett. 101 (2012) 111609, https://doi.org/10.1063/1.4752465.
[9] S. Baher, Z. Lorestaniweiss, Propagation of surface plasmon polaritons in monolayer graphene surrounded by nonlinear dielectric media, J. Appl. Phys. 124 (2018) 073103, https://doi.org/10.1063/1.5031191.
[10] T. Gric, O. Hess, Tunable surface waves at the interface separating different graphene-dielectric composite hyperbolic metamaterials, Opt. Express 25 (2017) 11466–11476, https://doi.org/10.1364/OE.25.011466.
[11] Z.Z. Alisultanov, R.P. Meilanov, Transport properties of epitaxial graphene formed on the surface of a superconductor, Semiconductors 48 (2014) 924–934, https://doi.org/10.1134/S1063782614070021.
[12] C.H. Gan, H.S. Chu, E.P. Li, Synthesis of highly confined surface plasmon modes with doped graphene sheets in the midinfrared and terahertz frequencies, Phys. Rev. B 85 (2012) 125431, https://doi.org/10.1103/PhysRevB.85.125431.
[13] H. Lu, C. Zeng, Q. Zhang, X. Liu, M.M. Hossain, P. Reineck, M. Gu, Graphene-based active slow surface plasmon polaritons, Sci. Rep. 5 (2015) 8443, https://doi.org/10.1038/srep08443.
[14] C. Li, X. Zhang, Y. Wang, Y. Song, D. Kong, Y. Wang, Slow surface plasmon polaritons with a large normalized delay bandwidth product in an ultracompact metal gap superlattice, Opt. Commun. 285 (2012) 1993–1996, https://doi.org/10.1016/j.optcom.2011.12.024.
[15] A. Vazquez-Guardado, G. Lopez-Galmiche, I. De Leon, R. Paez-Lopez, M. Torres-Cisneros, J.J. Sanchez-Mondragon, Slow surface plasmon-polaritons in a metal-dielectric structure incorporating a lorentzian gain medium, Latin America Optics and Photonics Conference (2012), https://doi.org/10.1364/LAOP.2012.LM2A.27.
[16] D. Fedyanin, A. Krasavin, A. Arsenin, A. Zayats, Surface plasmon polariton amplification upon electrical injection in highly integrated plasmonic circuits, Nano Lett. 12 (2012) 2459–2463, https://doi.org/10.1021/nl300540x.
[17] A. Abramov, I. Zolotovskii, S. Moiseev, D. Sementsov, Amplification and generation of surface plasmon polaritons in a semiconductor film – dielectric structure, Quant. Electron. 48 (2018) 22–28, https://doi.org/10.1070/QEL16487.
[18] L. Clampitt, Special issue on high-power microwave tubes, Proc. IEEE 61 (1973) 279–280, https://doi.org/10.1109/PROC.1973.9031.
[19] I. Zolotovskii, Yu Dadoenkova, S. Moiseev, A. Kadochkin, V. Svetukhin, A. Fotiadi, Plasmon-polariton distributed-feedback laser pumped by a fast drift current in graphene, Phys. Rev. A 97 (2018) 053828, , https://doi.org/10.1103/PhysRevA.97.053828.
[20] J. Liu, Di. Wang, S. Wu, M. He, L. Yu, X. Chao, G. Sun, Tunable plasmonic dispersion and strong coupling in graphene ribbon and double layer sheets structure, Plasmonics 12 (2017) 309–314.
[21] J. Liu, X. Zhai, F. Xie, L. Wang, S. Xia, H. Li, X. Luo, X. Shang, Analytical model of mid-infrared surface plasmon modes in a cylindrical long-range waveguide with double-layer graphene, J. Lightwave Technol. 35 (10) (2017) 1971–1979.
[22] L.A. Falkovsky, S.S. Pershoguba, Optical far-infrared properties of a graphene monolayer and multilayer, Phys. Rev. B 76 (2007) 153410, https://doi.org/10.1103/PhysRevB.76.153410.
[23] G.W. Hanson, Dyadic Green's functions and guided surface waves for a surface conductivity model of graphene, J. Appl. Phys. 103 (2008) 064302, https://doi.org/10.1063/1.2891452.
[24] E. Hajaj, O. Shtempluk, V. Kochetkov, A. Razin, Y. Yaish, Chemical potential of inhomogeneous single-layer graphene, Phys. Rev. B 88 (2013) 045128, , https://doi.org/10.1103/PhysRevB.88.045128.
[25] K. Lee, B. Fallahazad, J. Xue, D.C. Dillen, K. Kim, T. Taniguchi, K. Watanabe, E. Tutuc, Chemical potential and quantum Hall ferromagnetism in bilayer graphene, Science 345 (2014) 58–61, https://doi.org/10.1126/science.1251003.

[26] M. Sodha, A. Ghatak, Inhomogeneous Optical Waveguides, Plenum Press, New York, 1977.
[27] H. Lu, X. Gan, D. Mao, J. Zhao, Graphene-supported manipulation of surface plasmon polaritons in metallic nanowaveguides, Photonics Res. 5 (2017) 162–167, https://doi.org/10.1364/PRJ.5.000162.
[28] C. Li, X. Zhang, Y. Wang, Y. Song, D. Kong, Y. Wang, Slow surface plasmon polaritons with a large normalized delay bandwidth product in an ultracompact metal gap superlattice, Opt. Commun. 285 (2012) 1993–1996, https://doi.org/10.1016/j.optcom.2011.12.024.
[29] X. He, J. Fu, X. Fu, Y. Luo, R. Cheng, Analysis of mid-infrared graphene surface plasmons, Opt. Commun. 332 (2014) 149–153, https://doi.org/10.1016/j.optcom.2014.06.054.
[30] M.Z. Yaqoob, A. Ghaffar, M. Alkanhal, S. Rehman, F. Razzaz, Hybrid surface plasmon polariton wave generation and modulation by chiral-graphene-metal (CGM) structure, SC Rep. 8 (2018) 18029.
[31] D. Huang, A. Iurov, G. Gumbs, Role of electron back action on photons in hybridizing double-layer graphene plasmons with localized photons, J. Phys.: Condens. Matter 30 (2018) 204001.
[32] I. Suárez, A. Ferrando, J. Marques-Hueso, A. Díez, R. Abargues, P.J. Rodríguez-Cantó, J.P. Martínez-Pastor, Propagation length enhancement of surface plasmon polaritons in gold nano-/microwaveguides by the interference with photonic modes in the surrounding active dielectrics, Nanophotonics 6 (2017) 1109–1120 https://doi.org/10.1515/nanoph-2016-0166.